

AD-A172 299

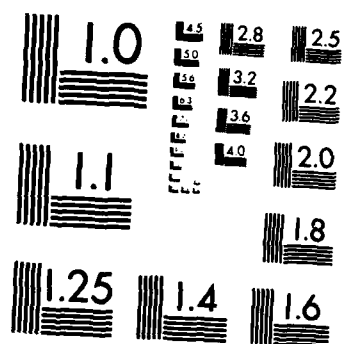
PH-SENSITIVE WO₃-BASED MICROELECTROCHEMICAL
TRANSISTORS(U) MASSACHUSETTS INST OF TECH CAMBRIDGE
DEPT OF CHEMISTRY M J NATAN ET AL 22 SEP 86 TR-11
N00014-84-K-0291 F/G 9/1

1/1

UNCLASSIFIED

NL





MICROCOPY RESOLUTION TEST CHART
NATIONAL BUREAU OF STANDARDS-1963-A

2

SECURITY CLASSIFICATION OF THIS PAGE (When Data Entered)

REPORT DOCUMENTATION PAGE		READ INSTRUCTIONS BEFORE COMPLETING FORM
1. REPORT NUMBER ONR TR 11	2. GOVT ACCESSION NO.	3. RECIPIENT'S CATALOG NUMBER
4. TITLE (and Subtitle) pH-Sensitive WO ₃ -Based Microelectrochemical Transistors		5. TYPE OF REPORT & PERIOD COVERED Interim Technical Report
		6. PERFORMING ORG. REPORT NUMBER
7. AUTHOR(s) Michael J. Natan, Thomas E. Mallouk, Mark S. Wrighton		8. CONTRACT OR GRANT NUMBER(s) N00014-84-K-0291
9. PERFORMING ORGANIZATION NAME AND ADDRESS Department of Chemistry Massachusetts Institute of Technology Cambridge, MA 02139		10. PROGRAM ELEMENT, PROJECT, TASK AREA & WORK UNIT NUMBERS Work Unit #202-261
11. CONTROLLING OFFICE NAME AND ADDRESS Office of Naval Research Department of the Navy Arlington, VA 22217		12. REPORT DATE September 22, 1986
		13. NUMBER OF PAGES 38
14. MONITORING AGENCY NAME & ADDRESS (if different from Controlling Office)		15. SECURITY CLASS. (of this report) unclassified
		15a. DECLASSIFICATION/DOWNGRADING SCHEDULE
16. DISTRIBUTION STATEMENT (of this Report) Approved for Public release; reproduction is permitted for any purpose of the United States Government; distribution unlimited.		
17. DISTRIBUTION STATEMENT (of the abstract entered in Block 20, if different from Report) Distribution of this document is unlimited		
18. SUPPLEMENTARY NOTES Prepared for publication in <u>Journal of Physical Chemistry</u>		
19. KEY WORDS (Continue on reverse side if necessary and identify by block number) molecular electronics, microelectrochemistry, microelectrodes, surface modification, molecule based transistors, polyaniline, poly-3-methylthiophene Chemical sensors, WO ₃ , pH-sensors		
20. ABSTRACT (Continue on reverse side if necessary and identify by block number) Attached		

DTIC
ELECTE
SEP 26 1986

S B D

AD-A172 299

DTIC FILE COPY

DD FORM 1 JAN 73 1473

EDITION OF 1 NOV 65 IS OBSOLETE
S/N 0102-LF-014-6601

SECURITY CLASSIFICATION OF THIS PAGE (When Data Entered)

ABSTRACT

Electrochemical properties of an array of closely spaced ($1.2\text{ }\mu\text{m}$) Au or Pt microelectrodes ($\sim 2\text{ }\mu\text{m}$ wide \times $\sim 50\text{ }\mu\text{m}$ long \times $0.1\text{ }\mu\text{m}$ high) coated by a $0.15\text{ }\mu\text{m}$ thick layer of polycrystalline WO_3 are reported. The WO_3 is deposited on the electrodes by rf sputtering of a WO_3 target. The cyclic voltammetry of these microelectrodes indicates that WO_3 connects individual microelectrodes, since the voltammogram of a pair of microelectrodes driven together is indistinguishable from that of an individual microelectrode. WO_3 becomes a good conductor upon electrochemical reduction in aqueous solutions. The change in resistance of WO_3 connecting two microelectrodes as a function of electrochemical potential spans four orders of magnitude, from $\sim 10^6$ to $\sim 10^2$ ohms. A pair of WO_3 -connected microelectrodes functions as a microelectrochemical transistor that is sensitive to pH. The cyclic voltammetry is pH-dependent and consistent with pH-dependent transistor characteristics, which indicate that the device is turned on at more positive electrochemical potentials in acidic media. In basic solutions, more negative potentials are needed to turn on WO_3 -based transistors. The maximum slope of the drain current, I_D , vs. gate voltage, V_G , plot at fixed drain voltage, V_D , gives a transconductance of 12 mS/mm of gate width. Potential step and potential sweep measurements indicate that the WO_3 -based transistor can be reversibly turned off and on in seconds; furthermore, the gate current, I_G , and I_D can be measured simultaneously, allowing demonstration of power gain for a sinusoidal variation of V_G at fixed V_D . Operating at a frequency of 1 Hz , the power amplification by the

WO₃-based transistor is 200, at pH 1. The power amplification decreases at both higher pH and higher frequency. The properties of the WO₃-based microelectrochemical transistor allow its use as a real-time pH sensor: a reproducible change in I_D , at fixed V_G and V_D , is obtained rapidly as the pH of a stream flowed continuously past the electrode is repetitively changed from pH 3.9 to pH 7.2.



Accession For	
NTIS GR&I	<input checked="" type="checkbox"/>
DTIC TAB	<input type="checkbox"/>
Unannounced	<input type="checkbox"/>
Justification	
By	
Distribution/	
Availability Codes	
Dist	Avail and/or Special
A-1	

pH-Sensitive WO₃-Based Microelectrochemical Transistors

Michael J. Natan, Thomas E. Mallouk, and Mark S. Wrighton*

Department of Chemistry

Massachusetts Institute of Technology

Cambridge, Massachusetts 02139

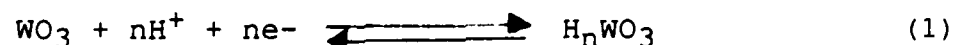
*Address correspondence to this author.

ABSTRACT

Electrochemical properties of an array of closely spaced ($1.2\text{ }\mu\text{m}$) Au or Pt microelectrodes ($\sim 2\text{ }\mu\text{m}$ wide \times $\sim 50\text{ }\mu\text{m}$ long \times $0.1\text{ }\mu\text{m}$ high) coated by a $0.15\text{ }\mu\text{m}$ thick layer of polycrystalline WO_3 are reported. The WO_3 is deposited on the electrodes by rf sputtering of a WO_3 target. The cyclic voltammetry of these microelectrodes indicates that WO_3 connects individual microelectrodes, since the voltammogram of a pair of microelectrodes driven together is indistinguishable from that of an individual microelectrode. WO_3 becomes a good conductor upon electrochemical reduction in aqueous solutions. The change in resistance of WO_3 connecting two microelectrodes as a function of electrochemical potential spans four orders of magnitude, from $\sim 10^6$ to $\sim 10^2$ ohms. A pair of WO_3 -connected microelectrodes functions as a microelectrochemical transistor that is sensitive to pH. The cyclic voltammetry is pH-dependent and consistent with pH-dependent transistor characteristics, which indicate that the device is turned on at more positive electrochemical potentials in acidic media. In basic solutions, more negative potentials are needed to turn on WO_3 -based transistors. The maximum slope of the drain current, I_D , vs. gate voltage, V_G , plot at fixed drain voltage, V_D , gives a transconductance of 12 mS/mm of gate width. Potential step and potential sweep measurements indicate that the WO_3 -based transistor can be reversibly turned off and on in seconds; furthermore, the gate current, I_G , and I_D can be measured simultaneously, allowing demonstration of power gain for a sinusoidal variation of V_G at fixed V_D . Operating at a frequency of 1 Hz , the power amplification by the

WO₃-based transistor is 200, at pH 1. The power amplification decreases at both higher pH and higher frequency. The properties of the WO₃-based microelectrochemical transistor allow its use as a real-time pH sensor: a reproducible change in I_D , at fixed V_G and V_D , is obtained rapidly as the pH of a stream flowed continuously past the electrode is repetitively changed from pH 3.9 to pH 7.2.

In this article we report the properties of WO_3 -based microelectrochemical transistors prepared by derivatization of microelectrode arrays with polycrystalline WO_3 , which undergoes the reversible, proton-dependent redox reaction shown in equation (1).¹



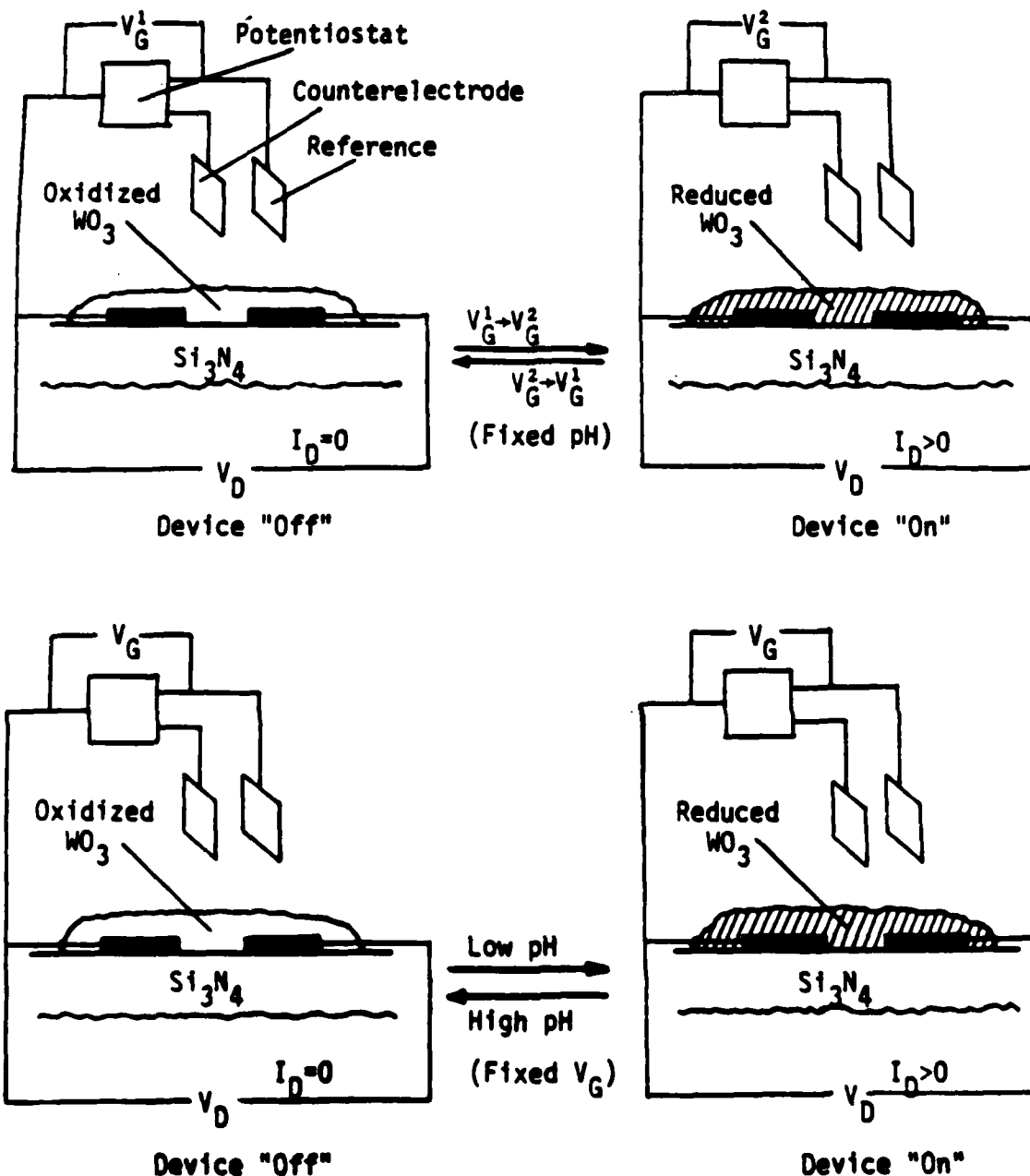
The microelectrode arrays were coated by rf plasma deposition from a sintered polycrystalline target of WO_3 . WO_3 has received considerable attention in recent years as an electrochromic material, because it becomes colored upon reduction.² In addition, reports on anodically grown,³ polycrystalline,⁴ colloidal,⁵ and dispersions of⁶ n-type semiconducting WO_3 have appeared. Further interest in the material stems from the fact that the reduced, cation-intercalated species, M_nWO_3 ($\text{M} = \text{H}^+$, Na^+ , and Li^+), are conducting.⁷ It is the change in conductivity of WO_3 and the pH dependence of the electrochemical potential where the conductivity occurs that is crucial in demonstrating a pH-dependent microelectrochemical transistor.

Closely spaced ($1.2 \mu\text{m}$) Au or Pt microelectrodes ($\sim 2 \mu\text{m}$ wide x $\sim 50 \mu\text{m}$ wide x $\sim 0.1 \mu\text{m}$ high) have proven useful to the study of electroactive, conducting organic polymers that can be derivatized onto Pt or Au.⁸⁻¹⁰ When the conductivity of the derivatized material can be modulated by control of the electrochemical potential of the redox active polymer, as in the cases of polypyrrole,⁸ poly(N-methyl pyrrole),^{8b} polyaniline,⁹ or poly(3-methylthiophene),¹⁰ the polymer-

connected microelectrodes behave as microelectrochemical transistors, in analogy to solid-state transistors.

A microelectrochemical transistor based on potential-dependent conductivity of a redox material is illustrated in Scheme I. When two closely spaced microelectrodes are connected by a redox active material such as WO_3 , the current which flows between the two microelectrodes (when there is a potential difference between them) can be modulated by a change in the redox state of the redox active material. The redox state is established by the gate potential, V_G . The charge needed to electrochemically switch the material between the insulating and conducting states is associated with the gate current, I_G . The potential difference between the two microelectrodes is called the drain voltage, V_D , and the current flowing in the drain circuit is I_D . When V_G is set to V_G^1 , the material is insulating, $I_D = 0$, and the device is off, but when V_G is moved to V_G^2 , the material becomes conducting, and the device is on, $I_D > 0$, for a fixed value of V_D . Polypyrrole,⁸ polyaniline,⁹ and poly(3-methylthiophene)¹⁰ are similar in that they are conducting when oxidized, and transistors based on these materials turn on at positive values of V_G . WO_3 , in contrast, is insulating when oxidized, and conducting when reduced (Scheme I). WO_3 -based transistors, then, are the first microelectrochemical devices which can be turned on at negative values of V_G relative to the saturated calomel reference electrode. The point is that turn on potentials are associated with reduction of the active material rather than with oxidation.

Another fundamental difference between WO_3 -based devices and the previously characterized microelectrochemical transistors is that the



Scheme I. A WO_3 -based transistor that turns on ($I_D > 0$) when V_G is moved from V_G^1 where WO_3 is oxidized and insulating to V_G^2 where WO_3 is reduced and conducting. The WO_3 -based device can also be turned on and off by varying the pH at fixed V_G .

reduction to the conducting state involves intercalation of cationic species (in aqueous solutions, protons) into the solid. This has two consequences, the first being that response time, the amount of time necessary to switch from the conducting state to the insulating state and back, is limited by the diffusion coefficient of protons within the oxide, which can be small.¹¹ The second consequence of the presence of H^+ in equation (1) is that the reduction of WO_3 is pH-dependent. Thus, the V_G required to turn on the device, V_G^2 , varies with pH. At a given V_G and V_D , a change in pH causes a change in the ratio of oxidized to reduced WO_3 , causing a change in I_D , as illustrated in Scheme I. Thus, a WO_3 -based microelectrochemical transistor functions as a pH sensor over a wide range of pH. Several other microelectrochemical transistors based on closely spaced microelectrodes connected by pH-sensitive electroactive materials have been developed by the Wrighton group,¹² including those based on platinized poly(3-methylthiophene),^{10b,13} a viologen/quinone polymer,¹⁴ and ferrocyanide-loaded, protonated poly(4-vinylpyridine).¹⁵ The system based on WO_3 -connected microelectrodes is the simplest, and operates over the widest range of pH's. Aside from WO_3 , there are many other transition metal oxides that could function in microelectrochemical devices. Nb_2O_5 ,^{2a,16} MoO_3 ,^{2a,17} IrO_2 ,¹⁸ and RhO_2 ^{18a,19} are examples of rugged oxides that can be switched electrochemically between conducting and insulating states by intercalation reactions similar to equation (1). A study of pH-sensitive $Ni(OH)_2$ -based microelectrochemical transistors has recently been completed.^{20,21}

EXPERIMENTAL SECTION

Preparation, Masking, Cleaning, and Encapsulation of Eight Wire Microelectrode Arrays. The microelectrode arrays used in these experiments were of a design described previously.⁸⁻¹⁰ The chips were masked prior to WO_3 deposition to ensure deposition on the array only either by manually applied aluminum foil masks or by photolithographically prepared Si_3N_4 masks $0.1\ \mu m$ thick. Immediately prior to deposition of WO_3 , the masked devices were cleaned by an O_2 plasma using a Harrick Plasma Cleaner. The chamber containing the samples was evacuated and backfilled with O_2 to a pressure of 160 microns. The plasma was formed and the samples were treated for 10 min. After deposition of WO_3 , electrical contact to individual wires was made and the devices were encapsulated in the usual fashion.^{8c}

Deposition of WO_3 . The deposition of WO_3 was accomplished using a modification of a literature procedure.²² Polycrystalline WO_3 was sputtered downhill from a sintered polycrystalline WO_3 target onto half-masked macroscopic Au, Pt, and SnO_2 electrodes, and onto masked microelectrodes using an R. D. Matthis SP 310 RF diode sputtering system. The power was provided by an RF Plasma Products power supply. The diameter of the cathode was 3.5 inches. The samples were initially presputtered for 15 minutes for further cleaning. Deposition then took place onto the heated (676K) samples for 8 to 12 minutes, depending on the thickness of WO_3 desired. The sputtering gas was a 10% O_2 /Ar mixture for both the presputtering and the actual deposition. These conditions allowed preparation of many samples

simultaneously, all having a coating of WO_3 of thickness 0.1-0.2 μm (depending on the sputtering time).

Measurement of Sample Thickness. Step profiles on WO_3 microelectrodes were measured using either a Tencor Instruments Alpha-Step 100 or a Sloan Dektak surface profiling system. Both macroscopic electrodes and microelectrodes gave the same thickness ($\pm 20\%$) for a given deposition. Step heights as small as 0.03 μm were measurable under favorable conditions.

Chemicals and Solutions. The H_2O used for all experiments was Omnisolv HPLC grade. The electrolytes were all commercially available and used as obtained. Unbuffered solutions, when used, were rigorously deoxygenated and kept under N_2 in order to maintain a constant pH value.

Equipment. Electrochemical experiments were performed using Pine Instruments RDE-4 bipotentiostats and Kipp and Zonen X-Y-Y' or X-Y recorders for microelectrodes and a PAR 173/175 potentiostat/programmer in conjunction with a Houston 2000 X-Y recorder for macroscopic electrodes. The Kipp and Zonen recorders or Tektronix storage oscilloscopes with camera attachments were used for time based experiments. A sinusoidal waveform was obtained using the internal oscillator output of a PAR 5204 lock-in amplifier. UV-visible spectra were recorded using either a Hewlett-Packard Model 8451-A diode array spectrophotometer or a Cary 17 spectrophotometer. Optical micrographs of microelectrodes were obtained with a Polaroid camera mounted on a Bausch and Lomb Model optical microscope. Reproducible chemical signals were delivered to microelectrodes using the two pumps of a Hewlett-Packard Model 1084B high pressure liquid chromatograph.

RESULTS AND DISCUSSION.

Characterization of RF Sputtered Films of WO_3 on Macroscopic Electrodes. The electrochemistry of thin films of polycrystalline WO_3 on optically transparent SnO_2 electrodes was examined at pH 4.5. As expected for the WO_3 electrochromic material,² intense coloration in the visible region accompanies electrochemical reduction, as shown in Figure 1. The significant changes in the absorbance at 700 nm occur from -0.3 to -0.8 V vs. SCE, where reduction is observed by cyclic voltammetry. The inset to Figure 1 shows the actual spectra after subtraction of the optical spectrum of the completely oxidized electrode. No significant spectral changes occur beyond -1.0 V vs. SCE for WO_3 at pH 4.5. The electrochemical potential of the cyclic voltammetric wave (and of coloration) moves with pH: at pH 0, less reducing potentials are needed to reduce the WO_3 , while basic solutions necessitate more reducing potentials to reduce the WO_3 .

Potential step measurements confirm that charge can be reversibly added to and withdrawn from WO_3 . At pH 4.5, integrated currents from potential steps from +0.6 V to more reducing potentials indicate that at potentials negative of -0.4 V vs. SCE, "metallic" behavior is obtained, as judged by linearity of charge vs. potential plots on macroscopic SnO_2 and Au electrodes.¹⁰ The data indicate that WO_3 has a capacity of approximately 100 F/cm³, somewhat smaller than that for poly(3-methylthiophene).¹⁰

Cyclic Voltammetry of WO_3 -Coated Microelectrodes. The cyclic voltammetry of arrays of microelectrodes coated with a 0.15 μm layer of WO_3 is depicted in Figure 2. The voltammograms we obtain on SnO_2 ,

Au, and Pt macroelectrodes have the same shape as those in Figure 2 for the microelectrodes. In all cases the cyclic voltammetry is invariant with time in acidic, neutral, and basic solutions. The shape of cyclic voltammograms of WO_3 have been modelled by Reichman *et al.*¹¹ Their results indicate that the shape depends, among other factors, on k_f , the charge transfer rate constant, and on the hydrogen atom diffusion coefficient within the film, D_H .¹¹ Our data is consistent with a material having a small D_H ($\sim 1 \times 10^{-9} \text{ cm}^2/\text{sec}$) and k_f ($\sim 10^{-2} \text{ sec}^{-1}(\text{mole}/\text{cm}^3)^{-2}$). The consequences of small values for D_H and k_f are a slow response time (manifested as a delay in oxidation of reduced WO_3 upon scan reversal). Anodically grown WO_3 , which has rapid response time, has larger values for both D_H ($\sim 5 \times 10^{-8} \text{ cm}^2/\text{sec}$) and k_f ($\sim 7.2 \text{ sec}^{-1}(\text{mole}/\text{cm}^3)^{-2}$).¹¹

Notwithstanding the irregularly shaped cyclic voltammetry, the importance of the data in Figure 2 rests in the fact that it shows that adjacent microelectrodes of the array are electrically connected with WO_3 and that charge transport within the oxide is rapid compared to the scan rate. At a given sweep rate, the cyclic voltammograms of wire A, wire B, and of wires A and B driven together are identical. The point is that all of the electroactive WO_3 is addressable by each wire; if the wires were not electrically connected, or if charge transport were slow on the timescale of the voltage sweep (as can be the case with a slow oxide like $\text{Ni}(\text{OH})_2$ ^{20,21} or a redox polymer⁸), the cyclic voltammogram of the two wires driven together would equal the sum of the individual voltammograms. At sufficiently thin coatings ($< 0.05 \mu\text{m}$), rf sputtered or thermally grown²¹ polycrystalline WO_3 does

not connect adjacent wires and the array behaves as eight individually addressable microelectrodes.

Integration of the voltammograms in Figure 2 indicates roughly 6×10^{-8} C is associated with the electrochemical process upon scanning from +0.2 to -0.4 V vs. SCE. Assuming that the density of WO_3 on the microelectrodes is that of the pure material, and that the surface area of WO_3 on the microelectrode array is $7 \times 10^{-9} \text{ m}^2$ (five times the area bounded by the wires themselves), and further assuming a one electron reduction per WO_3 unit, one can calculate that, as a lower limit, approximately 2.5% of the total quantity of WO_3 in electrical contact with the wires is reversibly reduced and reoxidized in a single scan from +0.2 to -0.4 V vs. SCE.

Resistance of WO_3 as a Function of Electrochemical Potential. The resistance of WO_3 connecting two (or more) microelectrodes can be measured by bringing both electrodes to a given V_G , and then scanning the potential of one microelectrode a small voltage ($\sim \pm 25$ mV) about V_G . The drain voltage, V_D , is the potential difference between the two electrodes developed by scanning one microelectrode. The current passing between the electrodes can be related to the resistance using Ohm's law. By varying V_G , resistance versus V_G can be assessed.

Figure 3 shows representative resistance vs. V_G data for a WO_3 -coated microelectrode array at pH 6.6. The top part of the figure illustrates the I_D - V_D curves for ± 25 mV potential excursions (at 5 mV/sec) around the gate voltage, V_G . The drain current is equal to zero for $V_D = 0$, and the resistance is taken to be the reciprocal of the slope at this point. The data in Figure 3(b) indicate that the resistance changes by over three orders of magnitude from 0.0 to -0.9

V vs. SCE at pH 6.6. For particular samples, the resistance may reach limits of just over 10^2 and 10^7 ohms, but the resistance of the material never changes by more than four orders of magnitude in aqueous solution. Thus, unlike the conducting organic polymers polyaniline⁹ and poly(3-methylthiophene),¹⁰ WO_3 does not exhibit very high resistance in the insulating state. The resistivity of as deposited WO_3 is extremely dependent on deposition conditions, varying from 10^3 ohm-cm to 10^9 ohm-cm.^{2b} Since polycrystalline WO_3 is an n-type semiconductor, the conductivity of the material is expected to be reasonably high in electrolyte-containing solutions, where the concentration of potentially doping impurities is high.

The ruggedness of the oxide, relative to conducting organic polymers,⁸⁻¹⁰ is evidenced by the stability of the material in the fully reduced (conducting) state. Excursions to -1.5 V vs. SCE, 250 mV negative of the V_G of maximum conductivity (at pH 7), do not cause any irreversible damage to the oxide; in contrast, if poly(3-methylthiophene), for example, is brought to an oxidizing potential substantially more positive than where the maximum conductivity is found, irreversible chemical oxidation occurs and the polymer is degraded.¹⁰

pH-Dependence of the Transistor Properties of WO_3 -Connected

Microelectrodes. The dependence on pH of the reduction of WO_3 causes the transistor properties of WO_3 -connected microelectrodes to also vary with pH. We have characterized the properties of WO_3 -based transistors as a function of pH. The left side of Figure 4 illustrates the cyclic voltammetry of WO_3 -connected microelectrodes at acidic, neutral, and basic values of pH. As expected by equation (1),

the reduction occurs at more negative potentials at basic pH, and at more positive potentials at acidic pH. In addition, there is a slight decrease in the amount of charge injected at basic pH, as reflected by integration of the voltammograms. When the pH is lowered, the cyclic voltammogram is identical to that obtained initially in acidic solution. There may be a reversible pH-induced structural change which blocks a percentage of WO_3 sites to reduction. The same phenomenon has been observed, to a greater extent, with $\text{Ni}(\text{OH})_2$ -coated microelectrodes.^{20,21} The right side of Figure 4 shows, at the same three pH's, linear plots of I_D vs. V_D (at fixed V_G) for several V_G 's, that also show a pH dependence. Thus, at $V_G = -0.2$ V vs. SCE, the device is completely turned off at pH 12.3 (judging from the lack of drain current for any V_D), slightly on at pH 6.6, and nearly fully turned on at pH 0. At a given pH, the slope of the I_D - V_D plots increases as V_G is moved negatively, again illustrating that the resistance between WO_3 -connected microelectrodes decreases as WO_3 is reduced.

Another way to quantitatively assess the effect of V_G on the conductivity of a WO_3 film is to measure I_D as a function of V_G , at a fixed V_D . The results of such a measurement, for three different values of pH, are plotted in Figure 5. The I_D - V_G characteristic, like the resistance- V_G plots of Figure 3 and the transistor curves in Figure 4, result from properties intrinsic to WO_3 : the values of V_G which give significant I_D , the maximum slope of the curve (the transconductance), and the maximum value of I_D (for a given V_D) may be expected to differ from material to material. As expected, the I_D - V_G curves depend on the pH. The maximum drain current obtained for a 200

mV drain voltage is 550 μ A, which exceeds that achieved with polypyrrole,⁸ or polyaniline,⁹ but is less than the 1 mA found for poly(3-methylthiophene)-based devices of the same geometry.¹⁰ The I_D for this particular device is approximately a factor of 5 higher than could be expected from the data in Figure 3, illustrating the sample to sample variability in resistance mentioned above. The reduced state of WO_3 is several orders of magnitude more conductive than the conducting (oxidized) state of $Ni(OH)_2$,^{20,21} indicating that a large variation in I_D - V_G characteristics may be found among metal oxide-based microelectrochemical devices. It is important to note that the maximum drain current of 550 μ A is achievable at pH \approx 7 by moving V_G to a strongly reducing potential; thus, at pH \approx 7 the entire I_D range of the device is accessible. Under basic conditions, an I_D of 550 μ A cannot be obtained at any V_G . The maximum slope of the I_D vs. V_G plot, transconductance, at pH 0, is around 12 mS/mm of gate width, an order of magnitude less than that obtained for poly(3-methylthiophene).¹⁰ At pH 6.6, the transconductance is approximately 10 mS/mm of gate width.

The data in Figure 5 illustrate how WO_3 might be used as a pH sensor, since a steady state measurement at fixed V_G and V_D gives an I_D which is solely a function of pH, presuming that other cations in solution, which are capable of intercalation into WO_3 ,⁷ do not interfere with the pH response. We have carried out several experiments to ascertain whether Li^+ , Na^+ , and K^+ affect the transistor behavior of WO_3 -based microelectrochemical devices, and find that their effect is minimal. For example, a WO_3 -based microelectrochemical transistor was placed in $\mu = 0.05$, pH 5 acetate

buffer with $V_G = 0.0$ V vs. SCE and $V_D = 150$ mV. A stable I_D of 265 nA was produced. Li^+ was added in the form of Li_2SO_4 to a concentration of 0.32 M. The I_D moved to 280 nA, a change of only ~6% for a four order of magnitude excess of interfering ion. Another experiment probed the effect of interfering ions on I_D - V_D plots for various V_G 's (Cf. Figure 4). Saturated KCl and NaCl solutions, and 2 M LiCl (all at pH 7) gave I_D - V_D plots identical to those obtained in 0.1 M Na_2SO_4 (at pH 7). Also, addition of base to a pH 0.5, 2 M LiCl solution caused the V_G for turn on to move to more reducing potentials. These experiments indicate that interference of K^+ , Na^+ , and Li^+ is negligible in WO_3 -based microelectrochemical transistors operated in aqueous solutions.

Microelectrochemical transistors are fundamentally different from solid state devices in that ionic movement is necessary to bring the material on a microelectrode to a conducting state. In the case of a solid state field effect transistor (FET), for example, source-drain current is merely a consequence of capacitative charging of the gate region, with no accompanying ionic movement.²³ Thus, ionic diffusion associated with faradaic processes places an upper limit on the on/off time for microelectrochemical transistors, and the response times can never be equal to those of solid state devices of the same dimensions. For the WO_3 used in this study, there are further limitations imposed by small values for k_f and D_H , as shown by the cyclic voltammetry in Figures 2 and 4. Thus, WO_3 -based microelectrochemical transistors exhibit response times slower than those of previously characterized microelectrochemical devices.⁸⁻¹⁰

Figure 6 shows data pertaining to the response time of a WO_3 -based transistor upon stepping from a potential of +0.4 V to 0.0 V vs. SCE, at pH 5. With a pulse width of 5 seconds, I_D varies between 0 and ~8.5 nA. The magnitude of I_D indicates that this particular sample of WO_3 was among the most resistive we have tested. The initial response time for both turn-on and turn-off is approximately 0.1 sec. After thirty minutes of continuous pulsing, there is deterioration in the response time, as I_D has lost a measure of rectangularity. After eight hours of continuous cycling, there is a very noticeable slowing of the response. The device neither turns fully on or off within the five second pulse width. In addition, the sluggish response is further manifested upon potential steps to more conducting states, where the completely on/completely off response time is measured in minutes, rather than seconds. It is possible that repeated potential steps on this particularly resistive sample caused structural changes which significantly affected k_f or D_H .

To the list of factors affecting response time of WO_3 -based transistors may be added the thickness of the oxide on the microelectrode array. The expectation that response time would improve as the quantity of derivatized WO_3 decreases is a realistic one, though at some point the connection between microelectrodes would be severed. Experiments with new microelectrode geometries will be undertaken to realize this expectation. For a given set of deposition conditions and a given thickness, a useful illustration of device response is the phase relationship of V_G , I_D , and I_G , depicted in Figure 7 at 1 Hz, at pH 1. V_G is varied sinusoidally from +0.5 V to -0.5 V vs. SCE at a frequency of 1 Hz. In theory, at 0.5 V vs. SCE, I_G

will always equal zero, as the device is fully off. Scanning negatively should result in cathodic current, I_G , associated with reduction of WO_3 in the gate region. Furthermore, I_G should also equal zero at -0.5 V vs. SCE, when the device is fully on, since all the electroactive WO_3 has been reduced. Scan reversal would then lead to anodic I_G associated with oxidation of the reduced WO_3 . At $+0.5$ V vs. SCE, the WO_3 is fully oxidized, and I_G is again zero. If I_G behaves ideally, then, it will be 90° out of phase with the $V_G(\text{peak})$. I_D should also be zero at $+0.5$ V vs. SCE, when the device is off, but should reach its maximum value at -0.5 V vs. SCE, when the device is expected to be fully turned on. Thus, I_D should be exactly in phase with V_G . Figure 7 shows that while I_D is in phase with V_G , I_G is slightly more than 90° out of phase with V_G . Even at 1 Hz, I_G cannot keep up with V_G . At higher frequency, I_D maintains its phase relationship to V_G more closely than does I_G , but leakage I_D (residual I_D when the device should be completely off), barely noticeable at 1 Hz, becomes quite prominent. In addition, the magnitude of I_D declines at higher frequency, indicating that the devices are not turning on fully. Results with conducting organic polymers derivatized on microelectrodes indicate that their behavior is a much closer approximation to ideal behavior at 1 Hz, and in some cases, much higher frequencies; polyaniline-based transistors can be switched on and off at frequencies up to 1 kHz.²⁴

The power amplification, A , observed for the data in Figure 7 can be calculated using equation (2), and is found to be 200, since

$$\underline{A} = \frac{\text{Average Power in drain circuit}}{\text{Average Power in gate circuit}} = \frac{P_{\text{drain}}}{P_{\text{gate}}} \quad (2)$$

$V_G(\text{peak}) = 1.0 \text{ V}$, $V_D = 0.5 \text{ V}$, $I_D(\text{peak}) = 44 \text{ } \mu\text{A}$, and $I_G(\text{peak}) = 0.11 \text{ } \mu\text{A}$. I_G is at best proportional to the scan rate, or switching frequency, and so \underline{A} decreases monotonically at higher frequencies. By 10 Hz, \underline{A} is reduced to 2; at 100 Hz, the charging current associated with I_G exceeds I_D and there is no power amplification ($\underline{A} < 1$). At these frequencies $I_G(\text{peak})$ continues to be more than 90° out of phase with $V_G(\text{peak})$, and $I_D(\text{peak})$ continues to be in phase with V_G , although its magnitude has declined and leakage current is significant. At pH > 1 , the response time of WO_3 -based transistors is slower. For example, at pH 7, a power amplification of 36 is obtained at 3×10^{-2} Hz, and power gain declines to 1 at less than 1 Hz.

While the power amplification and response time for WO_3 -based devices are much poorer than those of solid state devices,²³ the important result from Figures 4, 5, and 7 is that they show that WO_3 -connected microelectrodes are indeed chemically based transistors that function reproducibly. All the characteristics usually associated with conventional transistors, namely changes in the slopes of I_D vs. V_D plots as V_G is varied (Figure 4), sigmoidal plots of I_D vs. V_G at fixed V_D (Figure 5), and power amplification with well-behaved and separately measurable I_G and I_D (Figure 7), have been demonstrated. Thus, the analogy between solid state transistors and microelectrochemical transistors is complete; actuation by and

amplification of electrical signals has been achieved, though not on a competitive basis with solid state devices.

The possibility of achieving far better response time with WO_3 -based microelectrochemical transistors depends on two factors: improving deposition conditions and improving microelectrode geometry. Optimization of the deposition conditions with respect to response time for the WO_3 used in this work has been not been attempted. For instance, it is known that addition of H_2O to the plasma produces more porous, faster responsive films of WO_3 .² Undoubtedly, it is possible to derivatize microelectrode arrays with WO_3 that responds more quickly to changes in V_G . As mentioned above, a decrease in the amount of electroactive material used in connecting closely spaced microelectrodes will improve the response time. A method to achieve this without changing the thickness of WO_3 is to decrease the space between the wires of the microelectrode array. The technology to significantly close the $1.2\text{ }\mu\text{m}$ spacing currently in use, thereby reducing the volume of WO_3 required to contact microelectrodes, exists.²⁵ The volume of electroactive material needed in the gate region can further be reduced by coating the tops of microelectrodes with an insulating layer of Si_3N_4 .²⁴ Work is in progress to prepare microelectrode arrays of the improved geometry described. Even with the many improvements possible, chemically-based microelectrochemical transistors cannot ever achieve response times associated with solid state transistors, simply because ionic movement in the gate region of chemically-based devices cannot compete with electronic movement in the gate region of solid state devices. The potential utility of WO_3 -

based transistors rests in their ability to be turned on and off by a chemical signal, as in Scheme I.

Response of WO_3 -based Transistors to a Reproducible, Repetitive Change in pH in a Flowing Stream. The data in Figure 5 indicate that variation in I_D should be observed upon variation of pH in a solution in contact with a WO_3 -based transistor at fixed V_G and V_D . This fact, coupled with the durability of WO_3 in aqueous solutions (stable from pH 0-13; the material is soluble, however, in heated strongly basic solutions), and the lack of interference from cations, indicates that the device should make a good pH sensor. We have tested this possibility by using the two solvent reservoirs and pumps of an HPLC to create a flowing aqueous stream whose pH can be changed in order to deliver a reproducible pH change to the microelectrode. Using $\mu = 0.1$ M pH 7.2 phosphate buffer in one reservoir and $\mu = 0.1$ M pH 3.9 acetate buffer in the other, we can cycle the pH of the solution flowing past the WO_3 -coated microelectrode. The results of this experiment are shown in Figure 8, where $V_G = -0.5$ V vs. SCE, $V_D = 150$ mV, and the solvent flow rate is 6.0 ml/min. I_D is monitored over time and is found to be 0.08 μA for the pH 7.2 solution and 0.8 μA for the pH 3.9 solution. This I_D is less than what would be expected from Figure 5, but is consistent with the resistance data in Figure 3. The changeover from one pH to the other requires approximately 45 seconds; I_D reaches the steady state value within 90 seconds of when the transistor is exposed to the new pH solution. The stream was continuously flowed past the microelectrode for 6 h, without any degradation in the response time or the steady state I_D at either pH. Thus, a WO_3 -based transistor can sense changes in pH and gives large,

reproducible currents in real time. The magnitude of I_D is such that much smaller changes in pH should be detectable without further amplification of I_D .

CONCLUSIONS

The operation of pH-sensitive microelectrochemical transistors based on WO_3 -connected microelectrodes has been demonstrated. The response time of these devices is slower and power amplification is smaller than for microelectrochemical transistors based on conducting organic polymers, but the prospect of major improvements through control of deposition conditions and microelectrode geometry is possible. Unlike previously characterized microelectrochemical devices, the conducting region is accessed by negative values of V_G . This work shows that oxide-based transistors can be durable, and that, in principle, many oxides with widely varying properties can be used to fabricate microelectrochemical devices.

The effect of pH on the transistor behavior of WO_3 -connected microelectrodes has been probed; agreement with predictions based on the pH dependence of the electrochemical reduction of WO_3 has been found. Real-time I_D response, at fixed V_G and V_D , to pH change in a flowing stream has been shown. The full range of I_D is achievable at pH ≈ 7 through control of V_G . The transconductance of these microelectrochemical transistors is sufficiently large to insure significant I_D in the V_G range -0.25 to -0.8 V vs. SCE at pH ≈ 7 , where the redox potential of many biological reducing agents are found, meaning WO_3 -based devices may be of value in sensing biological molecules.

Acknowledgements. We thank the Office of Naval Research and the Defense Advanced Research Projects Agency for partial support of this research. Use of the rf sputtering facility at EIC Laboratories, Norwood, Massachusetts is gratefully acknowledged.

References

1. (a) Deb, S. K. Philos. Mag., 1973, 27, 807; (b) Faughnan, B. W.; Crandall, R. S.; Lampert, M. A. Appl. Phys. Lett. 1975, 27, 275; (c) Hersh, H. N.; Kramer, W. E.; McGee, J. H. Appl. Phys. Lett., 1975, 27, 646.
2. (a) Dautremont-Smith, W. C. Displays, 1982, 3, 3; (b) Agnihotry, S. A.; Saini, K. K.; Subhas Chandra Ind. J. of Pure and Appl. Phys., 1986, 24, 19.
3. (a) Di Quarto, F.; Di Paola, A.; Piazza, S.; Sunseri, C. Sol. Energy Mat., 1985, 11, 419; (b) Di Quarto, F.; Di Paola, A.; Sunseri, C. Electrochim. Acta, 1981, 26, 1177.
4. Desilvestro, J.; Neumann-Spallart, M. J. Phys. Chem., 1985, 89, 3684.
5. Nenadovic, M. T.; Rajh, T.; Micic, O. I.; Nozik, A. J. J. Phys. Chem., 1984, 88, 5827.
6. Erbs, W.; Desilvestro, J.; Borgarello, E.; Gratzel, M. J. Phys. Chem., 1984, 88, 4001.
7. (a) Dautremont-Smith, W. C.; Green, M.; Kang, K. S. Electrochim. Acta, 1977, 22, 751; (b) Crandall, R. S.; Faughnan, B. W. Phys. Rev. Lett., 1977, 39, 232.

8. (a) White, H. S.; Kittlesen, G. P.; Wrighton, M. S. J. Am. Chem. Soc., 1984, 106, 5375; (b) Kittlesen, G. P.; White, H. S.; Wrighton, M. S. J. Am. Chem. Soc., 1984, 106, 7389; (c) Kittlesen, G. P. Ph.D. Thesis, Massachusetts Institute of Technology, Cambridge, MA, 1985.
9. Paul, E. W.; Ricco, A. J.; Wrighton, M. S. J. Phys. Chem., 1985, 89, 1441.
10. (a) Thackeray, J. W.; White, H. S.; Wrighton, M. S. J. Phys. Chem., 1985, 89, 5133; (b) Thackeray, J. W. Ph.D. Thesis, Massachusetts Institute of Technology, Cambridge, MA, 1986.
11. Reichman, B.; Bard, A. J.; Laser, D. J. Electrochem. Soc., 1980, 127, 647.
12. Wrighton, M. S.; Thackeray, J. W.; Natan, M. J.; Smith, D. K.; Lane, G. A.; Belanger, D. Phil. Trans. Royal Soc., Ser. B, submitted.
13. Thackeray, J. W.; Wrighton, M. S. J. Phys. Chem., submitted.
14. Smith, D. K.; Lane, G. A.; Wrighton, M. S. J. Am. Chem. Soc., to be submitted.
15. Belanger, Daniel; Wrighton, M. S. J. Phys. Chem., to be submitted.

16. (a) Dyer, C. K.; Leach, J. S. J. Electrochem. Soc., 1978, 125, 23; (b) Reichman, B.; Bard, A. J. J. Electrochem. Soc., 1980, 127, 241.
17. (a) Arnoldussen, T. C. J. Electrochem. Soc., 1976, 123, 527; (b) Rabelais, J. W.; Colton, R. J.; Guzman, A. M. Chem. Phys. Lett., 1974, 29, 131; (c) Colton, R. J.; Guzman, A. M.; Rabelais, J. W. J. Appl. Phys., 1978, 49, 409; (d) Dickens, P. G.; Birtill, J. J. J. Electron. Mat., 1978, 7, 679.
18. (a) Dautremont-Smith, W. C. Displays, 1982, 3, 67; (b) Buckley, D. N.; Burke, L. D. J. Chem. Soc. Faraday Trans. I, 1975, 71, 1447; (c) Gottesfeld, S.; McIntyre, J. D. E.; Beni, G.; Shay, J. L. Appl. Phys. Lett., 1978, 33, 208.
19. (a) Gottesfeld, S. J. Electrochem. Soc., 1980, 127, 272; (b) Burke, L. D.; O'Sullivan, E. J. M. J. Electroanal. Chem., 1978, 93, 11.
20. Natan, M. J.; Belanger, D.; Carpenter, M. K.; Wrighton, M. S., manuscript in preparation.
21. Natan, M. J. Ph.D. Thesis, Massachusetts Institute of Technology, Cambridge, MA, 1986.
22. Miyake, K.; Kaneko, H.; Suedomi, N.; Nishimoto, S. J. Appl. Phys., 1983, 54, 5256.

23. Sze, S. M. "Physics of Semiconductor Devices"; Wiley: New York, 1981.

24. Lofton, E. P.; Thackeray, J. W.; Wrighton, M. S. Science, submitted.

25. (a) Mackie, S.; Beaumont, S. P. Solid State Technology, 1985, 28, 117; (b) Elliot, D. J. "Integrated Circuit Fabrication Technolgy"; McGraw-Hill: New York, 1982.

Figure Captions

Figure 1. Optical spectral changes at 700 nm accompanying the change in potential of an optically transparent SnO_2 electrode coated with a film of rf plasma-deposited polycrystalline WO_3 of 0.15 micron thickness. The electrolyte was a 0.1 M, pH 4.5 acetate buffer. The inset shows the visible range absorption spectra as a function of electrochemical potential.

Figure 2. Cyclic voltammetry at four sweep rates of adjacent wires of a WO_3 -coated microelectrode array driven individually and together in pH 6.6 phosphate buffer.

Figure 3. (a) Current-potential curves in pH 6.6 phosphate buffer as a function of V_G . The potential of one of the microelectrodes is varied by ± 25 mV around V_G , and I_D is measured. (b) The resistance between WO_3 -coated Au microelectrodes as a function of V_G , calculated from the slopes at $V_D = 0$ of the data in the upper portion of the figure.

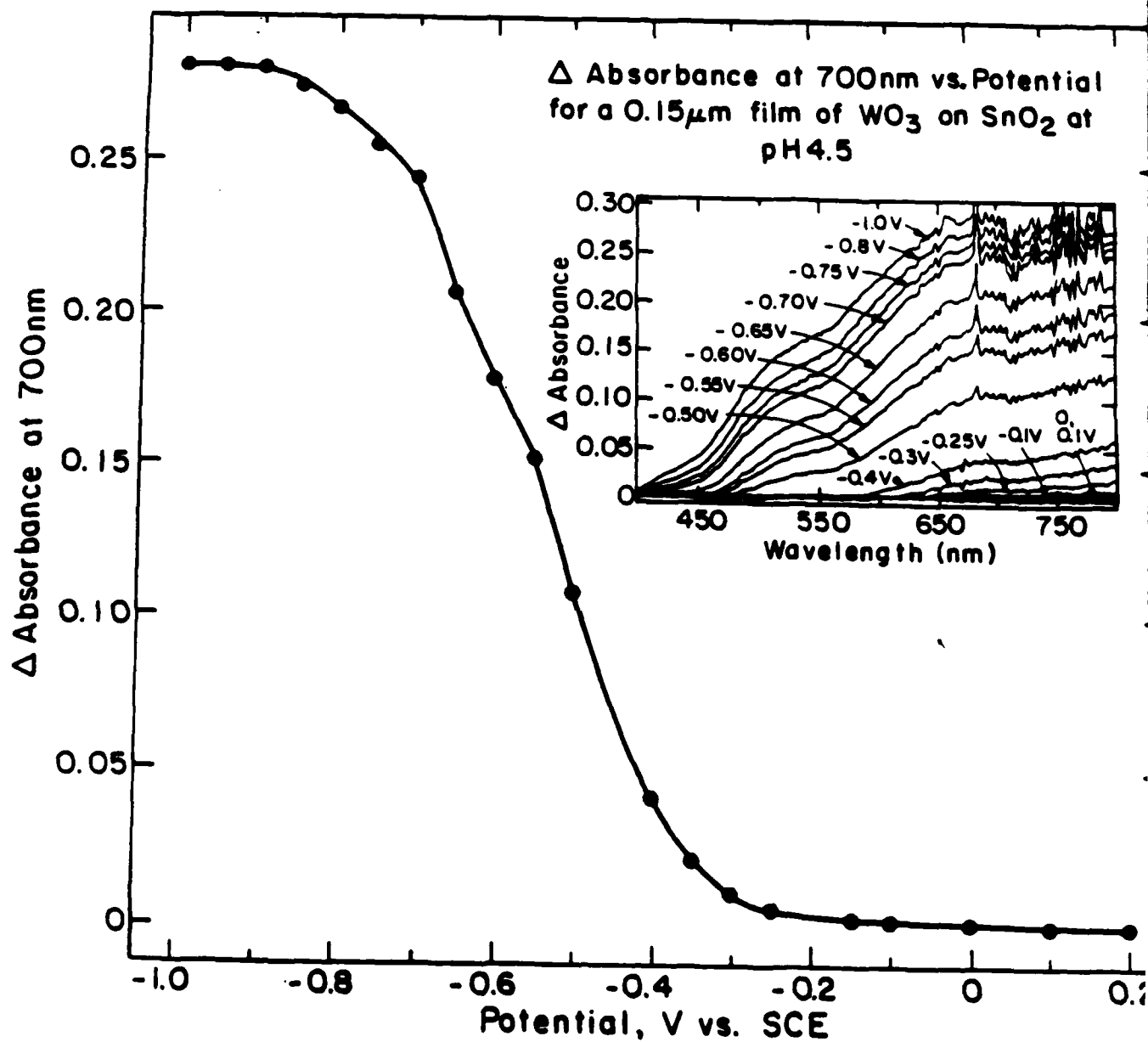
Figure 4. Cyclic voltammetry (left) and I_D vs. V_D (at fixed V_G) transistor characteristics (right) of WO_3 -connected microelectrodes at three different pH 's. The voltammograms were recorded at 200 mV/sec. V_D was varied at 10 mV/sec.

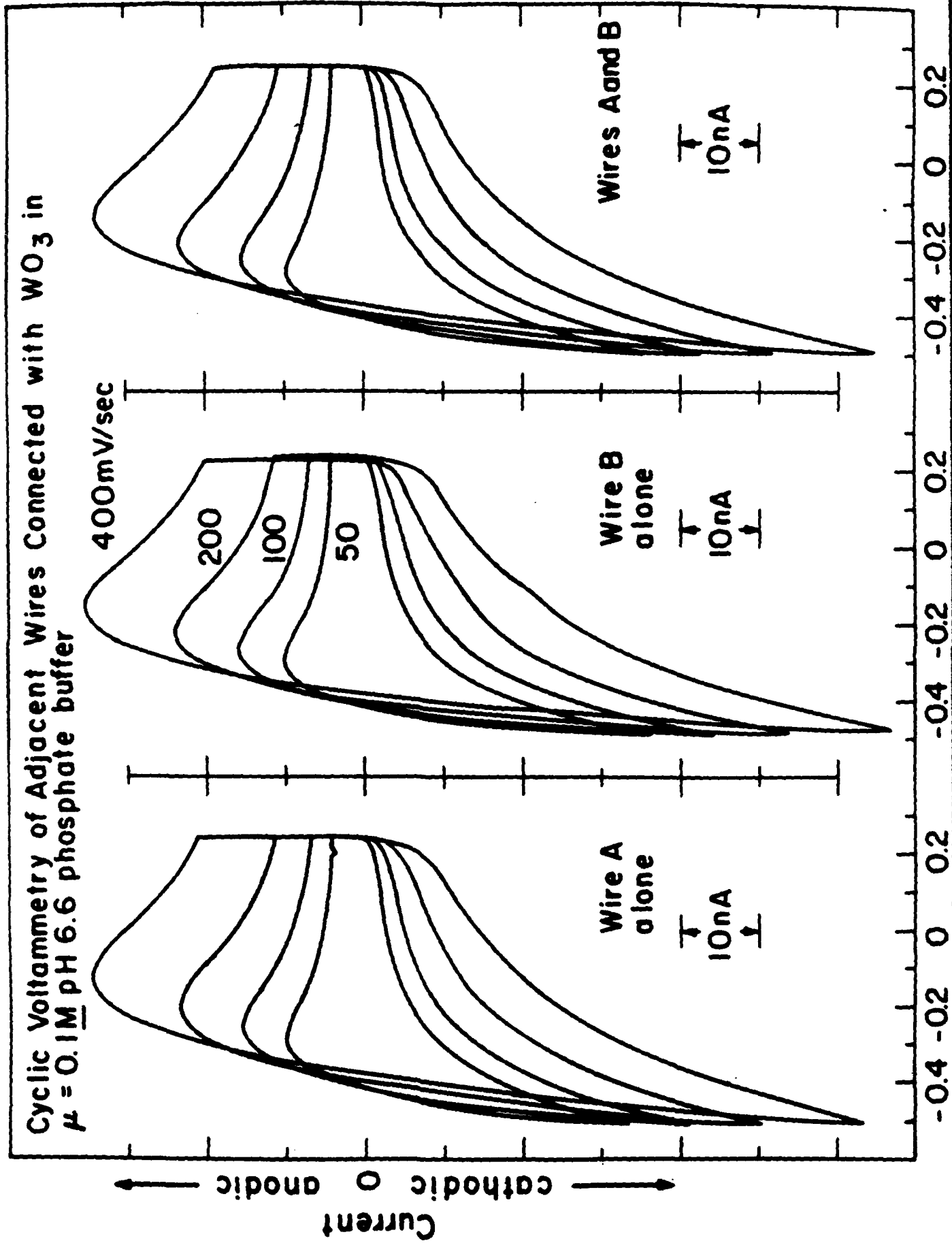
Figure 5. I_D vs. V_G at fixed (200 mV) V_D at three values of pH. These are steady state data.

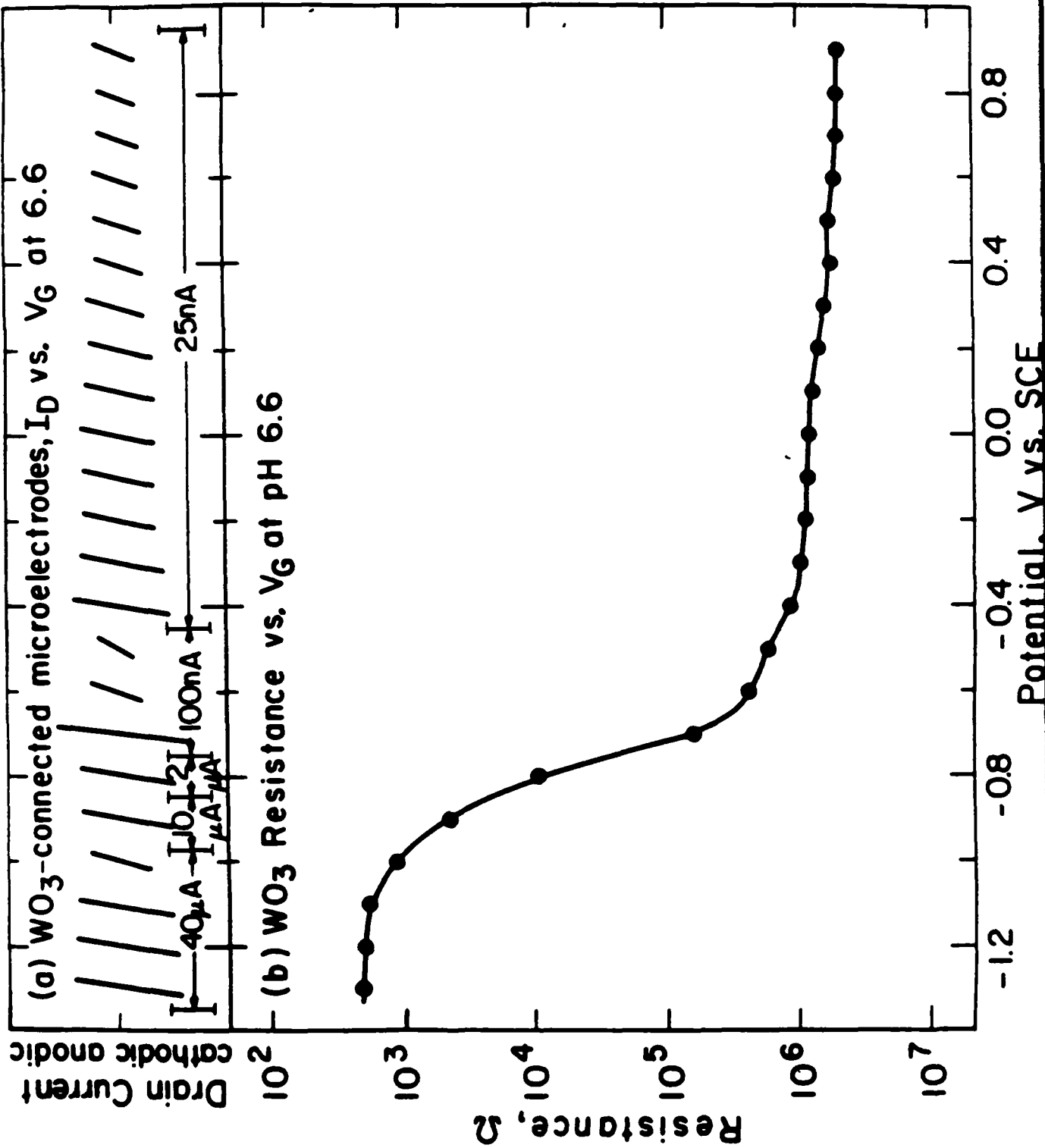
Figure 6. I_D vs. time for a WO_3 -based transistor at pH 5 for a potential step from +0.4 to 0 V vs. SCE.

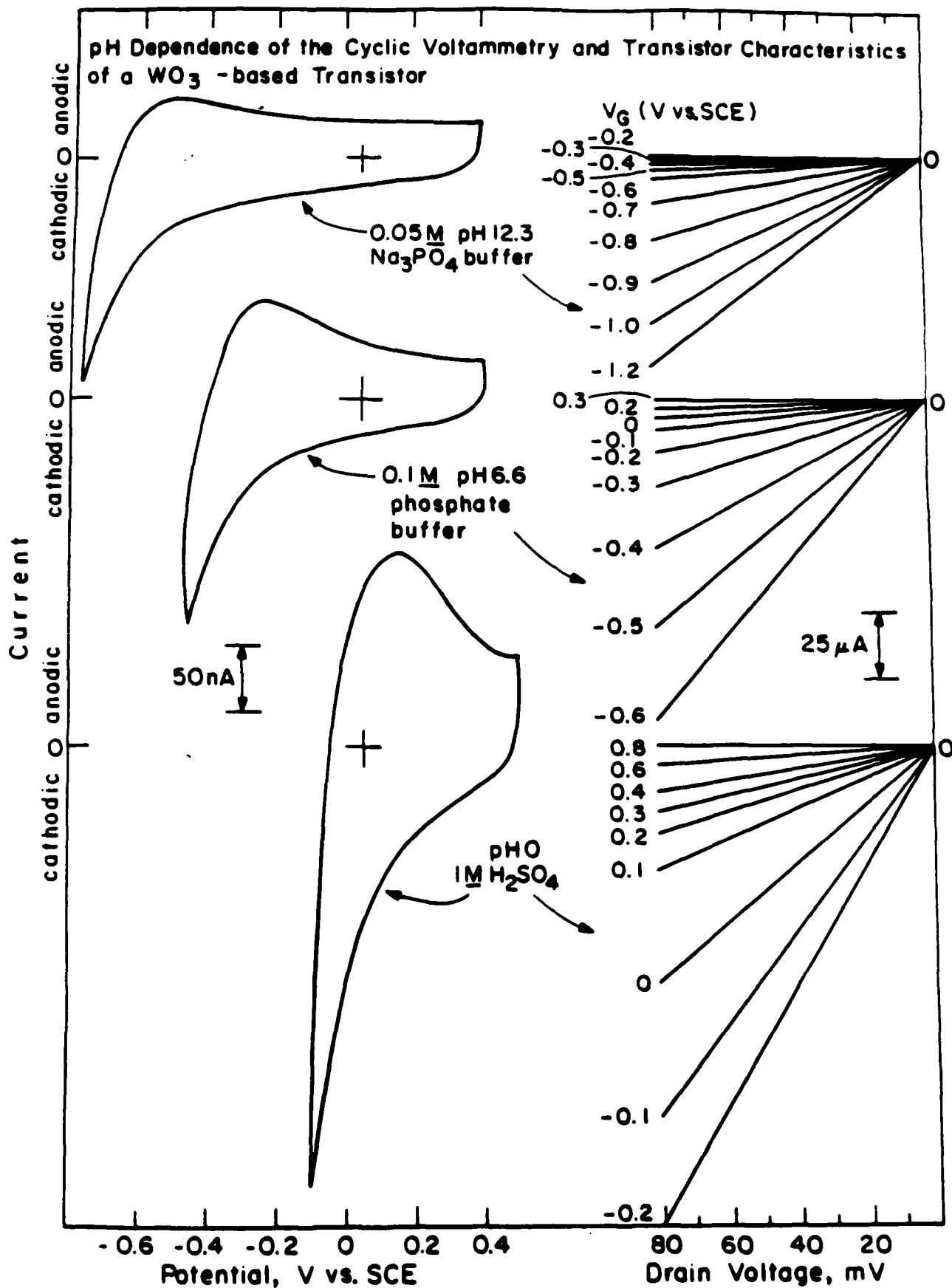
Figure 7. Phase relationship between V_G , I_G , and I_D for a WO_3 -based transistor at 1 Hz at pH 1. $V_D = 500$ mV. V_G was varied between +0.5 and -0.5 V vs. SCE.

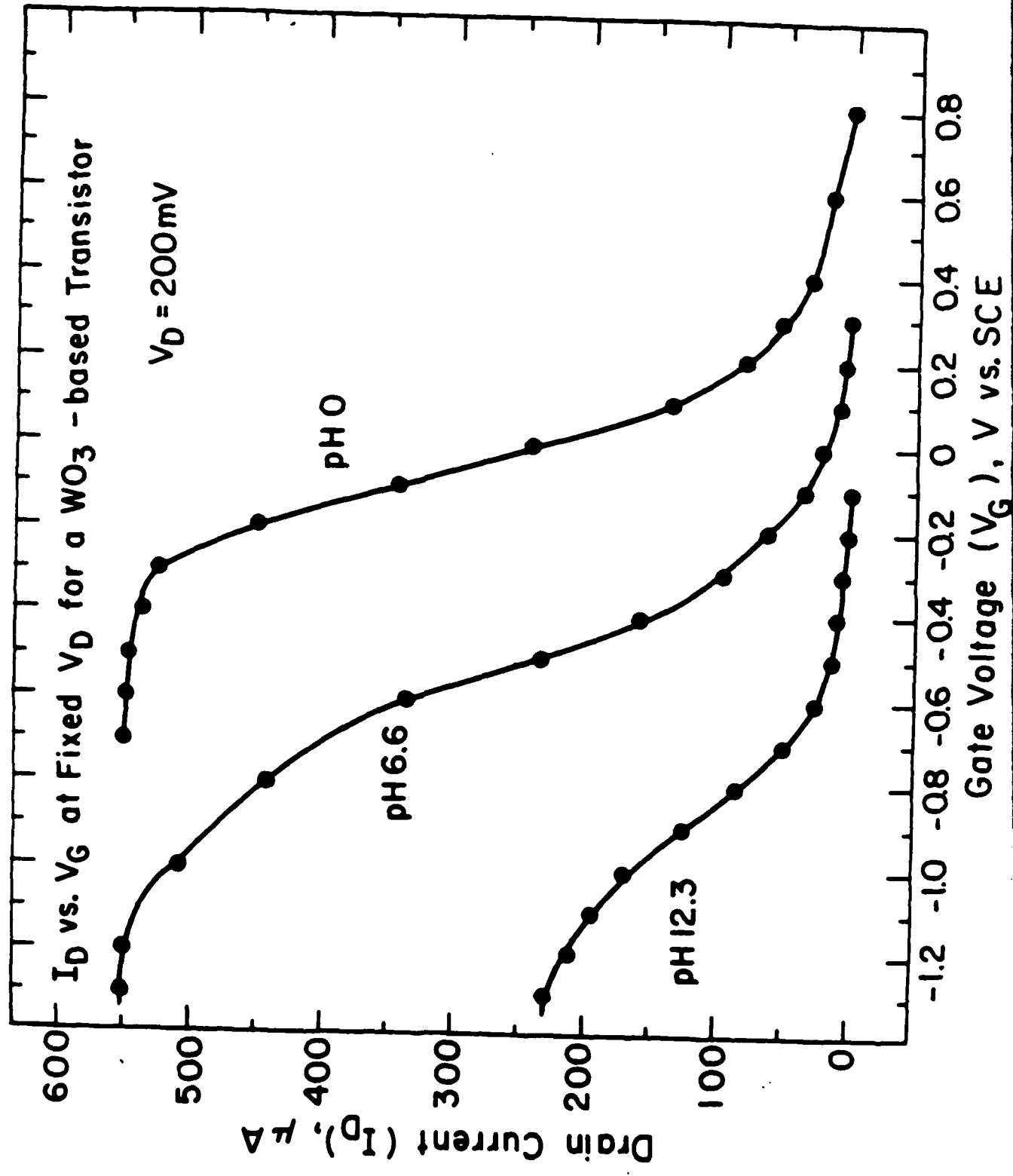
Figure 8. I_D vs. time for WO_3 -based transistor upon variation of pH in a continuously flowing stream. $V_G = -0.5$ V vs. SCE, $V_D = 150$ mV.



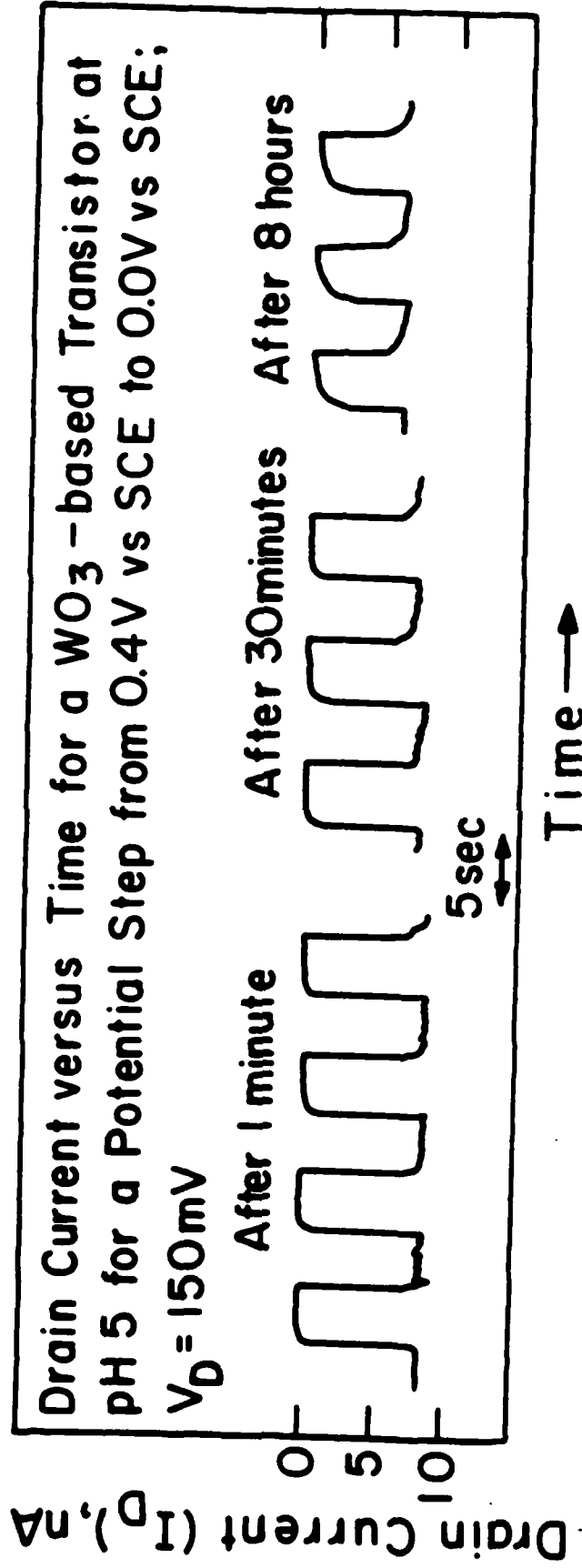




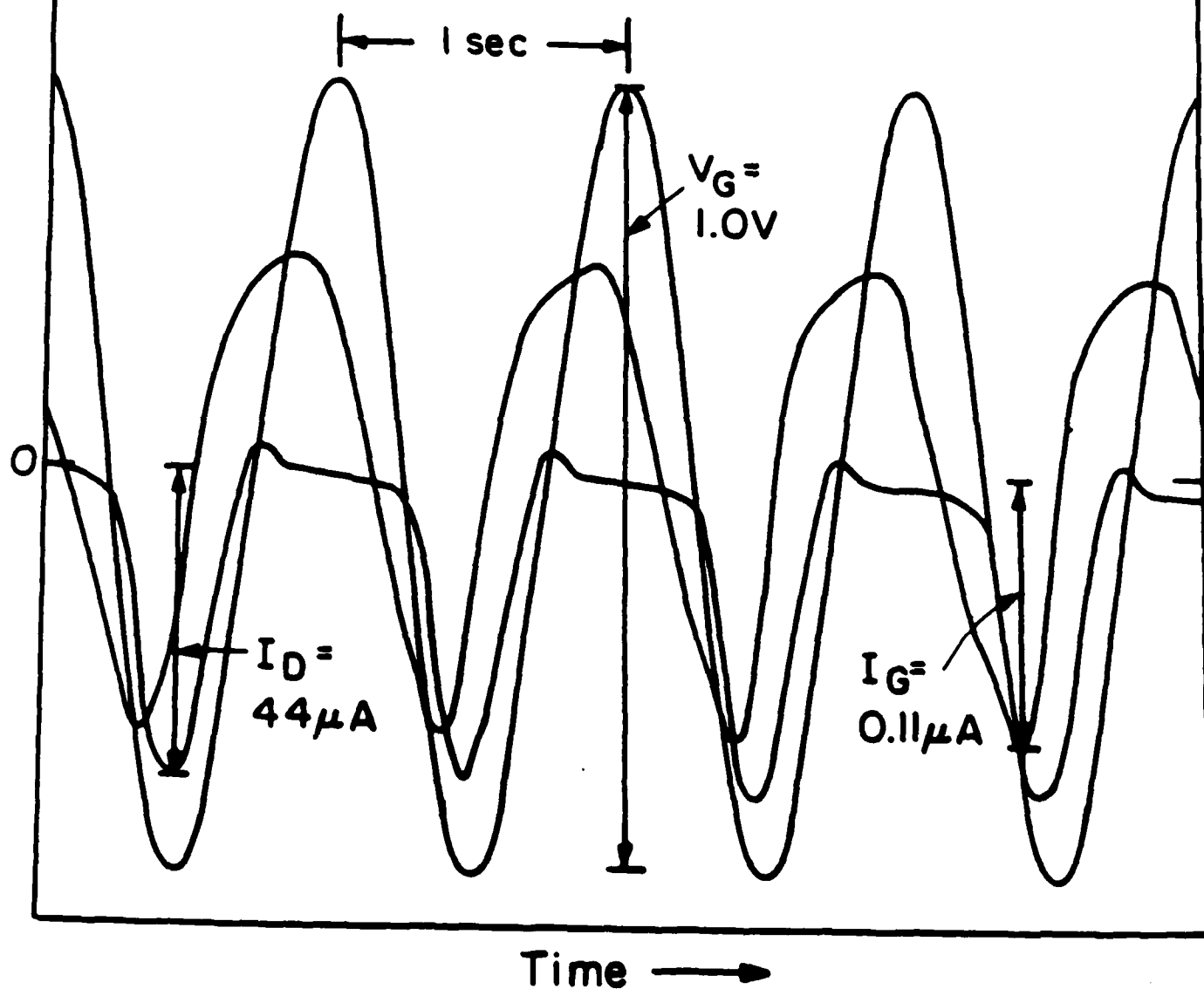


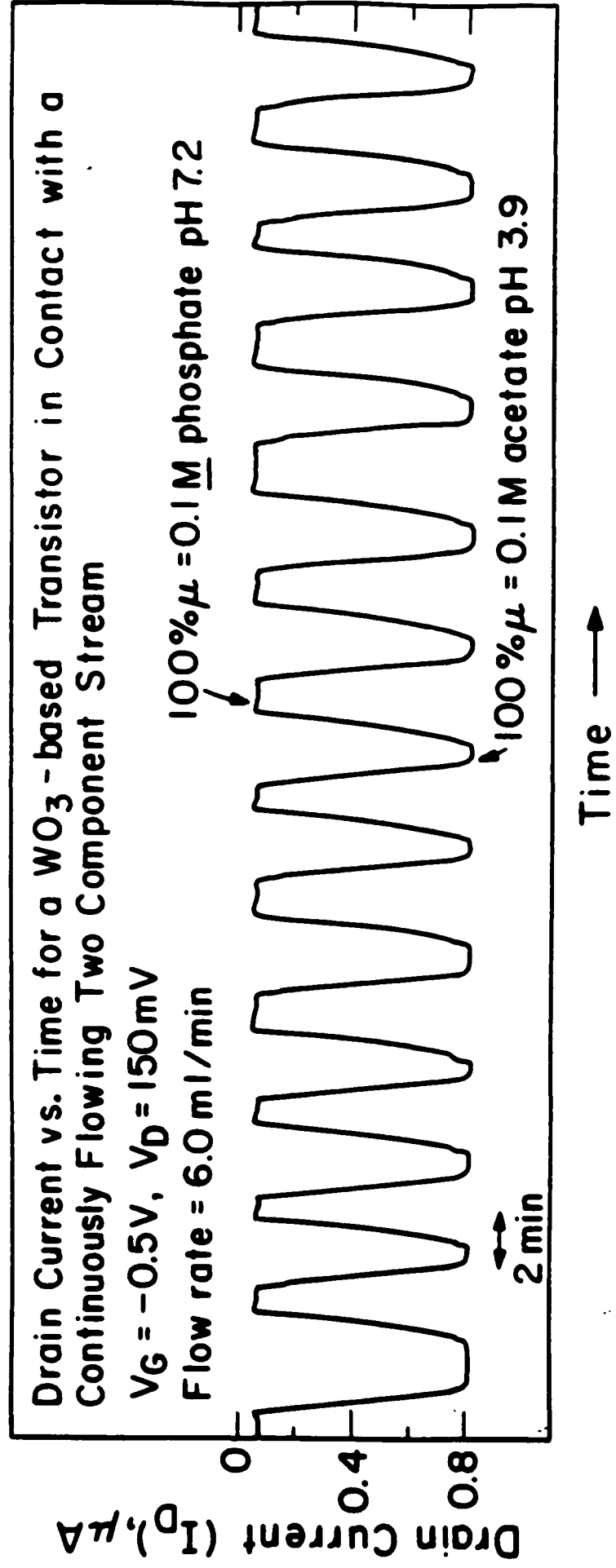


Drain Current (I_D), nA



Phase Relationship Between the Gate Voltage (V_G), Gate Current (I_G), and the Drain Current (I_D) at 1 Hz for a WO_3 -based Transistor at pH 1





DISTRIBUTION LIST

All Reports

Molecular Biology Program, Code 441MB
Office of Naval Research
800 N. Quincy Street
Arlington, VA 22217

Annual, Final and Technical Reports

Defense Technical Information Center (2 copies)
Building 5, Cameron Station
Alexandria, VA 22314

Annual and Final Reports Only (one copy each)

Scientific Library
Naval Biosciences Laboratory
Naval Supply Center
Oakland, CA 94625

Commanding Officer
Naval Medical Research & Development Command
National Naval Medical Center
Bethesda, MD 20814

Director
Infectious Disease Program Center
Naval Medical Research Institute
National Naval Medical Center
Bethesda, MD 20814

Commander
Chemical and Biological Sciences Division
Army Research Office
Research Triangle Park, NC 27709

Commander
U.S. Army Research and Development Command
Attn: SGRD-PLA
Fort Detrick
Frederick, MD 21701

Commander
USAMRIID
Fort Detrick
Frederick, MD 21701

Commander
Air Force Office of Scientific Research
Bolling Air Force Base
Washington, DC 20332

Administrative Contracting Officer
Office of Naval Research Laboratory
(address varies - obtain from Business Office)

Final and Technical Reports Only

Director, Naval Research Laboratory (6 copies)
Attn: Code 2627
Washington, DC 20375

END

10-86

DT/C